

WIDE ANGLE ANTENNA PATTERN MEASUREMENTS USING A POLY-PLANAR NEAR FIELD TECHNIQUE

Gregson S.F.^{1,2}, Parini C.G.², McCormick J.¹

BAE SYSTEMS¹ UK, Queen Mary, University of London² UK

ABSTRACT

For planar near-field methodology, if the forward hemisphere is to be determined exactly the propagating field must be sampled either in the aperture of the antenna or over a plane of infinite extent. In practice, due to the finite extent of the scan plane any conventional planar near-field measurement will inevitably represent a truncated data set, and as such, any predicted far-field pattern would include errors associated with this truncation. Furthermore, the precise nature of this effect is complicated, as a variation in any part of the near-field pattern will necessarily, as a consequence of the holistic nature of the transform, result in a change to every part of the corresponding far-field pattern.

However, it is the data that is transformed to produce the far-field pattern that is required to be free from excessive truncation. If this data is the product of the combination of a number of partial planar data sets that, in contrast to the single scan data set, fulfils the transformation requirements in terms of sampling rate and continuity over the sampling interval, then the prediction will be free from truncation errors.

Techniques for rigorously applying vector isometric rotations to antenna patterns and thereby correcting the measurements of misaligned antennas (1), readily offer the possibility of producing antenna measurements based upon partial scans that are *not* coplanar. By rotating the AUT about one or *more* spatial axes that are not necessarily at a normal to the scan plane and combining the partial scans, it is possible to increase the “angle of validity” of a planar measurement. This introduces the possibility of constructing bespoke polyhedral measurement surfaces that enclose the antenna under test and that are designed to be more amenable for the derivation of wide-angle antenna performance from measurements made using existing, possibly smaller, planar near-field measurement facilities. This technique facilitates a reduction in the number of near-field acquisition points, relative to a conventional planar measurement with an equal angle of validity, while retaining as much as possible of the mathematical and computational simplicity that is usually associated with the plane wave spectrum (PWS) method and planar probe pattern correction.

This paper will show through numerical simulation and experimental measurement that a flat-topped pyramid provides a possible solution to the measurement of high gain antenna patterns in the forward hemisphere using a planar scanner of size of order 1.5 times the size of the radiating aperture. Additionally it is shown

that by enclosing a medium gain antenna (*e.g.* a corrugated horn) within an imaginary box and measuring the near field on all six sides of the box, using a suitable rotation of the AUT, a prediction of the full spherical radiation pattern of the antenna can be obtained.

1. RECONSTRUCTION OF NORMAL COMPONENT

Conventionally the normal field components are not measured, instead they are recovered from the tangential components via an application of the plane wave condition, *i.e.* $\underline{k} \cdot \underline{E} = 0$. If however, the sampled data set is truncated, the reconstructed normal field component will be in error. This is clearly a problem as partial scans are by definition, truncated. Furthermore, this field component is required before the partial data sets can be combined, as the principal of superposition requires that each component be resolved onto the same polarisation basis. These difficulties can be resolved if the normal field component is sought over the surface of each partial plane. All three orthogonal field components can then be transformed to the far field whereupon the partial data sets can be combined in the usual way. Thus, the normal field component over the partial scan plane can be expressed mathematically as,

$$E_z(x,y) = -\mathfrak{T}^{-1} \left\{ \frac{k_x \mathfrak{T}\{E_x(x,y)\} + k_y \mathfrak{T}\{E_y(x,y)\}}{k_z} \right\} \quad (1)$$

Where \mathfrak{T} represents the 2D Fourier transform of the near-field on a plane and \mathfrak{T}^{-1} its inverse. Using the simulator the normal field component was obtained from the tangential components results from this comparison can be found presented below in figure 1.

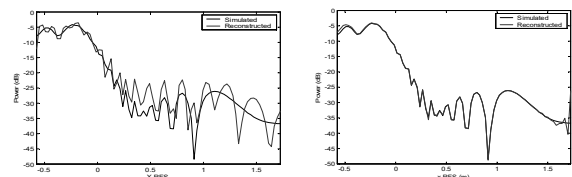


Figure 1 Plot of simulated and reconstructed normal field component without (a) and with (b) windowing

The spurious high frequency ripple that is present in the reconstructed normal field component can be removed by windowing the tangential field components before transforming to the angular spectrum. The “convoluted” normal spectral component can be obtained directly from equation 1 whereupon it can be inverse transformed to obtain the “windowed” normal field component. The windowing function can then be divided out to obtain reliable

results such as those presented in figure 1b. The derivation of the expressions that are used to correct the measured near field data for the directive properties of the measuring probe relied upon the validity of the plane wave condition. Thus, the normal field component utilised implicitly within these expressions will be recovered erroneously for the case where the near field data set is truncated. Thus, truncated measurements that are corrected with these expressions will also be in error. Again, such difficulties can be avoided with the application of a suitable windowing function.

Various windowing functions have been tried however of those tried the best results have been obtained by utilising a Bartlett *i.e.* a triangular, windowing function. At the extremities, this technique gradually becomes susceptible to noise and at the perimeter suffers from a divide by zero error. This can be overcome by over scanning the data where adjacent planes join. Figure 2 below shows a far field co-polar azimuth cut for a representative tri-scan auxiliary rotation configuration for a 0, 5, and 20 column over scan configuration.

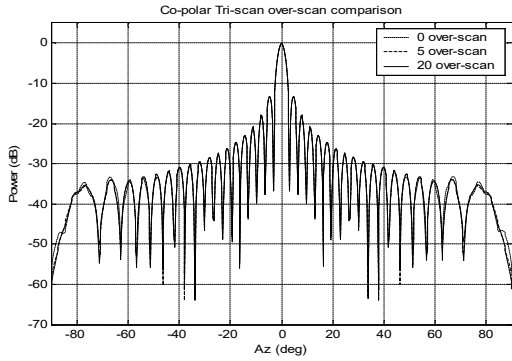


Figure 2 Comparison of far field horizontal cuts of polyhedral transform for various degrees of over scan.

Clearly, the over scan configurations improve the quality of the results obtained, this is most observable at wide angles however, an over scan of greater than five columns appears to offer only a very limited improvement.

Within the most general integral transform derivation of the PWS representation of electromagnetic fields (2), the partial derivatives of the boundary conditions with respect to the x -axis are obtained using the following operator substitution,

$$\frac{\partial u(x, y, z)}{\partial x} = \mathfrak{T}^{-1}\{-jk_x \mathfrak{T}\{u(x, y, z)\}\} \quad (2)$$

A similar expression can be obtained for the y partial derivative, and higher order derivatives were obtained by successive applications of these operator substitutions. These expressions were assumed to hold everywhere and were employed to reduce the scalar Helmholtz equation, which is a second order partial differential equation, to an ordinary differential equation. Unfortunately, if the boundary conditions are only piecewise smooth, the integration by parts that is

performed within the derivation of these operator substitutions becomes impossible. The implication of this is that the function must be considered as a distribution, *i.e.* a generalised function and crucially, any derivatives must also be considered as generalised derivatives. This can be easily demonstrated as far electric field in a half space at stationary points of the first kind, can be obtained rigorously, using spectral techniques, from near field data sampled over a non-planar aperture using (2),

$$E(r\hat{u}) = j \frac{e^{-jk_0 r}}{\lambda r} \iint_{-\infty-\infty}^{\infty} E(x, y, f(x, y)) e^{jk_0(\alpha x + \beta y + \gamma z)} (\hat{u} \cdot \hat{n}) \sqrt{\left(\frac{\partial g}{\partial x}\right)^2 + \left(\frac{\partial g}{\partial y}\right)^2 + 1} dx dy \quad (3)$$

Here, the surface profile is expressed as a function of the plaid, monotonic, and equally spaced co-ordinates x and y where $g(x, y, z) = z - f(x, y) = 0$, \hat{n} is the outward facing unit normal to the surface of integration and $\hat{u} = \alpha \hat{e}_x + \beta \hat{e}_y + \gamma \hat{e}_z$ is the unit vector in the direction of the stationary point. Here, provided the fields are sampled at, or preferable higher than, the Nyquist rate over the sampling surface, and provided the surface of integration is smooth, *i.e.* the function describing the surface profile, and all of the first partial derivatives are continuous, reliable far field data can be obtained. However, as soon as the surface profile is not smooth, as is the case for the poly planar technique, a spurious high frequency ripple can be observed. The amplitude of this ripple is dependent upon the magnitude of the ordinary discontinuity and the intensity of the field in that region. Although useful for electromagnetic modelling, and illustrates the difficulties inherent within the PWS method, these expressions are not in a form that is applicable for near field antenna measurements as no provision is made for probe pattern correction.

2. NEAR FIELD TO FAR FIELD TRANSFORM

Previously, a certain degree of success has been obtained by acquiring near field data over the surface of a flat-topped pyramid (3). Here, the intersection between adjacent scans can be chosen to be regions of lower field intensities, and the angle between scans could be made to be small, typically a few tens of degrees. However, in principal, these techniques only minimise, but do not remove the error inherent within the transformation technique. Consequently, an alternative technique that better handles discontinuities in the sampling surface was sought. To this end, the Kirchhoff-Huygens (KH) formula was utilised (4). Unlike the spectral method the KH method requires that both the Electric and Magnetic fields be known over the sampling surface. Thus, the filtered probe corrected PWS method can be utilised to correctly recover the normal component of the electric field and the magnetic field components can be reconstructed

over each of the partial scans. When combined, these partial scans form a conceptual finite but unbounded surface that encloses all of the current sources. This data can then be transformed to the far field using the KH method. Figure 3 below contains a block diagram of the novel hybrid spectral physical optics transformation algorithm.

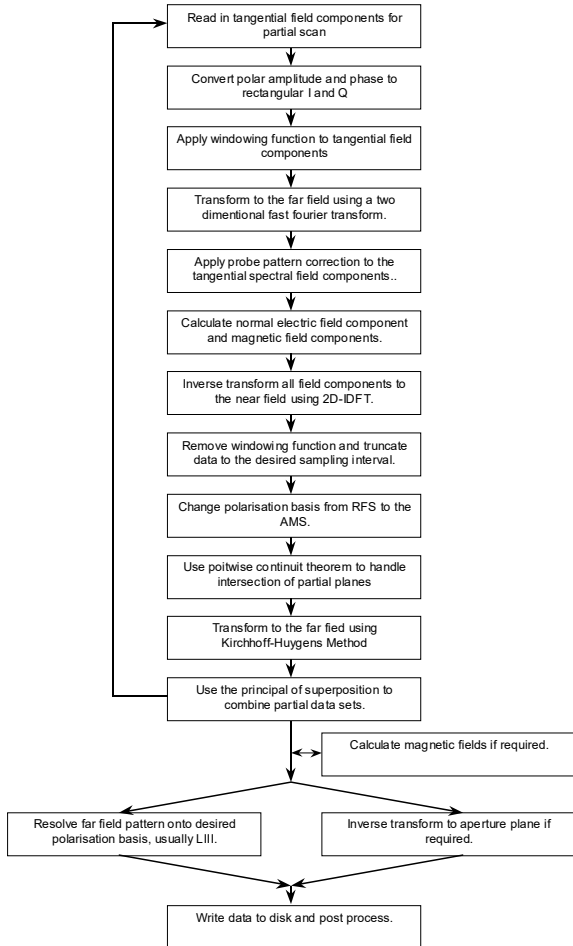


Figure 3 Block diagram of auxiliary rotation near field to far field transform algorithm.

3. EXPERIMENTAL VERIFICATION

A new purpose built high precision planar near field scanning (PNFS) facility has been installed and commissioned at QMUL. The QMUL PNFS is situated within an electromagnetically screened anechoic chamber. In contrast to other planar facilities an absorber has been placed throughout the chamber so as to minimise the scattering. The robotic positioner is of an inverted “T” design fabricated by Near-Field Systems Inc (NSI). This design was chosen in order that the scattering cross-section of the frame could be minimised. The relatively small physical dimensions of the scan plane, approximately 1m^2 , enable the planarity of the scanner to be maximised. Other advantages include minimising the length of the RF cabling within the facility. As highly phase stable cable is often relatively lossy, *i.e.* 1 dBm^{-1} , the short length of the cable runs enables the dynamic range of

the facility to be maximised, which is crucial, when the AUT is not nominally aligned to the axes of the range. Since the scanner is small and light it is also very fast with a maximum scan speed of 0.5 ms^{-1} thus acquisition times are short, typically of the order of a few minutes so very little thermal drift is present within a given acquisition. The RF subsystem is based around an HP8720 vector network analyser. The QMUL PNFS was partly funded by EPSRC under the JREI scheme.

In an attempt to verify the poly planar measurement and transformation methodologies a cubic geometry was adopted, as the orthogonality between adjacent partial scans would constitute a worst case scenario whilst being relative simple to realise. The AUT positioner was fabricated from a thin absorber clad steel column upon which the AUT could be mounted precisely in one of six discrete orientations. A relatively low gain corrugated horn was chosen as this class of antenna is conventionally thought to be unsuitable for characterisation by planar techniques.

The x - and y -polarised electric field components were sampled using a square acquisition window of $-0.425\text{m} \leq x_{RFS}, y_{RFS} \leq 0.425\text{m}$ with a range length, *i.e.* an AUT-to-probe separation, of 0.282m . Since the intention was that the tangential components of the near electric field were to be sampled over the surface of a cube, this corresponded to an over scan of 12 elements, *i.e.* approximately 6 wavelengths, around the perimeter of the square acquisition window. Once the x - and y -polarised near field components had been sampled the AUT was rotated by 90° in azimuth so the second side of the cube could be measured. All six surfaces of the cube were sampled by performing the following rotations from position 1: 1) AUT nominally aligned to axes of range, 2) positive rotation of 90° about y -axis, 3) negative rotation of 90° about y -axis, 4) positive rotation of 180° about y -axis, 5) positive rotation of 90° about z -axis, followed by a positive rotation of 90° about new x -axis, 6) positive rotation of 90° about z -axis followed, by a negative rotation of 90° about new x -axis. The requirement for the inclusion of the back plane follows from the requirement to perform the pattern integration over a *closed* surface. Although utilising the line charge distribution method (5), which is often referred to as Kirchhoff-Kottler formulation can ease these difficulties, this technique has not yet been implemented. In practice, this is not possible to achieve as a degree of truncation will inevitable result from the positioning system, this example was chosen to verify the transformation process, rather than the measurement process.

Each of the six partial scans were processed using the novel transformation algorithm schematically depicted in Figure 3 above. The y -polarised electric near field can be found plotted in figure 4 below, *i.e.* with reference to the fiducial co-ordinate system associated with the mechanical datum attached to the AUT. As

expected, the fields at the intersection between adjacent partial scans are continuous.

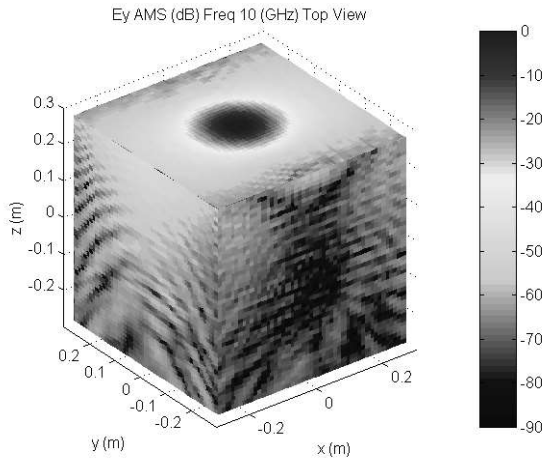


Figure 4 probe corrected y-polarised electric field component

Similarly encouraging results were obtained for other polarisation's and for the magnetic fields. These data sets were subsequently transformed to the far field and resolved onto a Ludwig III polarisation basis. Great circle cardinal cuts are shown in Figure 5 and 6.

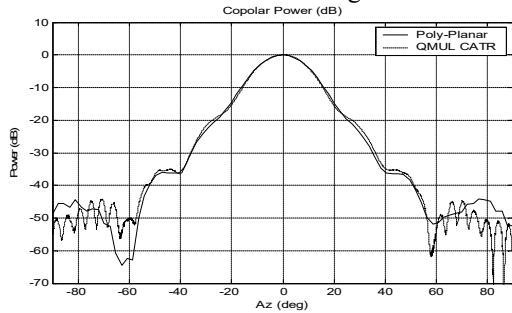


Figure 5 Azimuth great circle cut

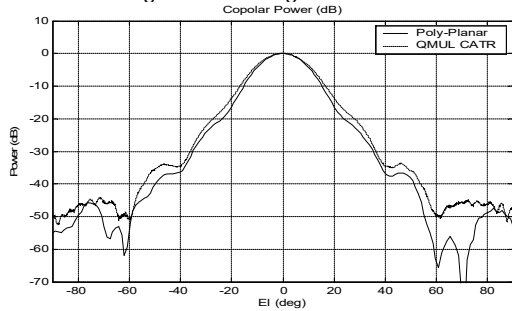


Figure 6 Elevation great circle cut

Here, the black traces represent patterns obtained from the poly-planar technique whilst the dashed traces denote results obtained from the QMUL compact antenna test range (CATR) (6). The high frequency oscillatory behaviour evident within the azimuth cut of the CATR at wide angles is a result of a multiple reflections within the facility and should be ignored. As described previously, the six partial planes will not intersect perfectly, and the adverse effects of reflections from scatters within the chamber will degrade the resulting far field patterns. Corrugated horns are renowned for their symmetry. Consequently, lack of symmetry can often be used as an indication that a measurement is unreliable. Here, although a good degree of symmetry can be observed in the azimuth plane, the elevation cut clearly contains a

number of asymmetries. This difference between the cardinal cuts is most probably an artefact of additional rotation required to sample the top and bottom planes of the cube, as the additional 90° rotation will inevitably introduce further alignment errors. Clearly, as the AUT is located at the centre of a conceptual measurement cube, classically the angle of validity for the front plane would be $\pm 45^\circ$ in azimuth and elevation. Thus, particular attention should be paid to regions around $\pm 45^\circ$ as if the transformation were in error, this is where it would be expected to be most noticeable. Crucially, no discernible divergence is observable in this region. Finally, the radial component of the far electric and magnetic fields were calculated. As expected these components were found to be reassuringly small with a peak signal of approximately 150 dB below the copolar peak.

4. FUTURE WORK AND CONCLUSIONS

This paper recounts the progress of an ongoing research study. Consequently, several issues remain to be addressed and the future work is to include:

1. Characterise a very low gain antenna, *e.g.* a waveguide probe to confirm the transformation when large field intensities illuminate the sidewalls of the measurement cube and confirm that larger field intensities at intersection between adjacent partial scans do not adversely affect the performance of the novel transform.
2. Orientate the conceptual measurement cube so that the boresight of the AUT intersects with one of the corners. This is a worst possible case and would illustrate that the orientation of the cube is unimportant.

The measurement process requires a great deal of refinement. However, for the first time encouraging results, that are free from the high frequency spurious ripples that have plagued *all* previous attempts, have been obtained. Thus, it would appear that probe corrected spectral techniques could be combined with the KH method to form a hybrid technique that alleviates the deficiencies that render these techniques useless when used individually.

REFERENCES

1. S.F. Gregson, J. McCormick, "Image Classification as Applied to the Holographic Analysis of Mis-Aligned Antennas", ESA ESTEC 1999.
2. S.F. Gregson, "Probe-Corrected Poly-Planar Near Field Antenna Measurements", Ph.D. Thesis, University of London, October 2002.
3. S.F. Gregson, C.G. Parini, J. McCormick, "Poly-Planar Near Field Antenna Measurements", Antenna Measurements and SAR, Loughborough, 28-29 May 2002.
4. R.H. Clarke, J. Brown, "Diffraction Theory and Antennas", Ellis Horwood Ltd, Chichester, 1980.
5. C.C. Chappas, "The Calculation of Aperture Radiation Patterns", Ph.D. Thesis, University of London, 1974.
6. A.D. Olver, C.G. Parini, "Millimetrewave Compact Antenna Test Ranges", JINA, November 1992, Nice.